Isomeric effects on the reactivity of branched alkenes: An experimental and kinetic modeling study of methylbutenes

Hwasup Song, Dongil Kang, Gina Fioroni, Goutham Kukkadapu, Yann Fenard, Nimal Naser, S. Scott Goldsborough, Roland Dauphin, Scott W Wagnon, William J Pitz, et al.

Isomeric effects on the reactivity of branched alkenes: An experimental and kinetic modeling study of methylbutenes

Hwasup Song[1,a)], Dongil Kang[2], Gina Fioroni[3], Goutham Kukkadapu[4], Yann Fenard[1], Nimal Naser[3], S. Scott Goldsborough[2], Roland Dauphin[5,b)], Scott W. Wagnon[4], William J. Pitz[4], Charles K. Westbrook[4], Guillaume Vanhove[1,*]

[1] Univ. Lille, CNRS, UMR 8522 - PC2A - Physicochimie des Processus de Combustion et de l'Atmosphère, Lille F-59000, France

[2] Transportation and Power Systems Division, Argonne National Laboratory, Lemont, IL, 60439, USA

[3] Center for Integrated Mobility Sciences, National Renewable Energy Laboratory, Golden, CO, 80403, USA

[4] Materials Science Division, Lawrence Livermore National Laboratory, Livermore, CA 94551, USA

[5] TOTAL Marketing Services, Centre de Recherche de Solaize, Chemin du Canal – BP 22, Solaize 69360, France

* Corresponding author : guillaume.vanhove@univ-lille.fr
a) Current address: Department of Mechanical Engineering, Kumoh National Institute of Technology, 61 Daehak-ro, Gumi-si, Gyeongsangbuk-do 39177 KOREA
b) Current address : CONCAWE Boulevard du Souverain 165, B-1160 Brussels –Belgium.

Abstract

A detailed experimental study of the low-to-intermediate temperature combustion of methylbutene isomers, i.e., branched C_5 alkenes, has been undertaken with multiple experimental facilities. Ignition delay times were measured at equivalence ratios 0.5–2.0, 685–1020 K and up to 45 bar condition from two rapid compression machines and showed slight deviation from an Arrhenius behavior for all three isomers, while their reactivity order differs as temperature changes. Sampled intermediates formed during the oxidation process of mixtures at 900–1150 K and 0.82 bar from a flow reactor and at 730 K and 20 bar from a rapid compression machine were analyzed using gas chromatography techniques. Trends in the formation and consumption of sampled intermediates were modeled using a kinetic model developed in this work for all three isomers. Rate of production and sensitivity analyses emphasize the role of double bond-specific reactions governing the global reactivity of these fuels. Additional studies of the addition reactions of HO_2 radicals to the double bond and to allylic radicals may improve the model performance.

1. Introduction

Conventional transportation fuels consist of multiple hydrocarbon families, e.g., alkanes, alkenes, cycloalkanes, aromatics, etc., whose combustion behavior under engine-relevant conditions is highly dependent on their reaction kinetics. Among these families, alkenes are of special interest thanks to their high research octane number (RON) and large octane sensitivity (S), making them promising blendstocks for advanced fuels designed for highly boosted and downsized SI engines [1–6]. In US gasolines, C_5 to C_7 alkenes are most common with branched alkenes being more prevalent because of their higher octane rating [7]. Alkenes also are formed in significant quantities during the oxidation of alkanes, making the development of accurate kinetic models for their oxidation relevant to simulations of alkane fuel components or alkane mixtures [8,9] in fuel-rich conditions.

Despite their role in the combustion chemistry of alkanes as intermediates, the oxidation kinetics of alkenes are not yet satisfactorily described in the low-to-intermediate temperature combustion regime [10]. For example, continued efforts on the comprehensive kinetic modeling of larger alkanes such as isooctane (2,2,4-trimethylpentane) [11–13] and *n*-heptane [14] have been quite successful, while the most notable recent progress on branched alkene models concern isobutene [10,15], 2-methyl-2-butene [16,17], high-temperature combustion models of 2-methyl-1-butene [18], methylbutene isomers [19,20] and tetramethylene [21]. Some literature is available for linear alkenes, e.g. 1-pentene [22,23], 1- and 2-pentene [24], linear hexene isomers [9,25–27] and linear heptene isomers [28–30]. Notably, studies of the kinetics responsible for the ignition of the isomers of hexene have demonstrated the relationship between the double bond position and the global reactivity. It was observed that the global reactivity towards ignition is inhibited as the C=C double bond moves towards the center of the molecule [9,22,24,25,29]. For larger branched alkenes, e.g. diisobutylene isomers, only one kinetic model focused on its high temperature chemistry was available [31] until the late 2010s; within the last 3 years, comprehensive kinetic modeling studies for 2,4,4-trimethyl-1-pentene [32] and both 2,4,4-trimethyl-1- and -2-pentene [33] have been conducted. In addition to that, intermediate species formed under the low-temperature combustion regime were experimentally observed [34] and theoretical calculation

results are also now available on their elementary reaction rates [35,36]. These previous efforts revealed that the specific reaction pathways relevant to the C=C double bond have a significant impact on the global reactivity of alkenes at low temperatures, inhibiting the reaction pathways responsible for the typical low temperature ignition of alkanes. Theoretical studies have also advanced our knowledge towards understanding this specific reaction chemistry [37–40]. Detailed experimental measurements such as speciation under engine-relevant conditions are essential in validating kinetic models but are largely absent from the literature.

This study focuses on the low-to-intermediate temperature combustion kinetics of branched C_5 alkenes—namely 2-methyl-1-butene (2M1B), 2-methyl-2-butene (2M2B), and 3-methyl-1-butene (3M1B), as shown in Fig. 1. These are all C_5 branched alkenes that are commonly present in US gasolines. Among them, 2M2B has drawn more attention due to its structure where 9 of 10 C-H bonds are allylic [16]. The presence of so many allylic C-H bonds makes 2M2B a very attractive candidate to study resonance stabilized radical kinetics and the influence of the carbon-carbon double bond on short alkyl chains. For example, Ray and Waddington conducted a speciation study of 2M2B and 2,3-dimethylbutene using a static reactor and discussed their oxidation processes at 550 K [41]. The authors identified major intermediate species, e.g., 3-methyl-3-hydroxy-2-butanone, 2-methyl-3-hydroxy-1-butene, 3-buten-2-one, 2-methylpropenal, 2-butanone, and 3-methyl-3-buten-2-one from 2M2B. A kinetic model for the oxidation of 2M2B was proposed by Westbrook et al. [16] and validated with jet-stirred reactor speciation results obtained at 600–1100 K and shock tube experiments over 1330–1730 K at various pressures and equivalence ratios. No negative temperature coefficient (NTC) behavior was observed by Westbrook et al. [16] and their findings were corroborated by Yin et al. [39] in their jet-stirred reactor oxidation and pyrolysis experiments for 2M2B. A recent high-temperature shock-tube and kinetic modeling study also stressed the need for detailed studies of 3M1B in the low- to intermediate-temperature regime [18]. Finally, very recently, laminar flame speeds and ignition delay times were measured at high temperatures for 2M1B and 2M2B [42].

Figure 1: Chemical structures of the studied isomers. 2M1B: 2-methyl-1-butene, 2M2B: 2-methyl-2-butene, 3M1B: 3-methyl-1-butene.

In this study, a self-consistent, comprehensive oxidation model of the methylbutene isomers is proposed and validated using new ignition delay time (IDT) measurements from rapid compression machines (RCMs) over a wide temperature and pressure range, along with speciation measurements from an RCM and a flow reactor.

2. Experimental setup

2.1. NREL flow reactor

Methylbutene isomers were purchased from Sigma-Aldrich and were ≥ 98% pure. Analysis was performed in a straight quartz tube flow reactor that is open to the atmosphere and operates under ambient laboratory conditions in Golden, Colorado, USA, (i.e., approximately 0.82 bar). The reactor has been described previously [43]; a brief description follows. The reactor consists of a tube that is 762 mm in length and is housed inside a temperature-controlled ceramic furnace with a heated zone length of 711 mm. Helium is utilized as the inert gas carrier and is introduced at the inlet of the reactor along with oxygen and fuel via a glass Y-union. The fuel is delivered at 10 µL/min via a syringe pump, and the helium and oxygen gases are introduced through mass flow controllers. The helium flow was reduced to maintain a constant residence time δ = 0.35 s as the temperature is increased, resulting in a progressive increase in the fuel and O_2 mole fraction as the reactor temperature increases, as visible in Figs. 3-5. The oxygen flow was maintained to impose an equivalence ratio of 1. The details of all the conditions investigated for each isomer and obtained experimental results are provided as Supplemental Material. The effluent of the reactor is sampled directly into an inert gas sampling line that is held at 75°C to avoid condensation of the collected species inside the line. Gas is drawn into the sampling line using a vacuum pump that feeds two identical sample loops in two separate GC systems that are used to measure and characterize the sampled species. GC1 is equipped with two identical 60m x 0.25 µm x 0.25 µm DB-1 columns (Agilent Technologies) for simultaneous analysis of C4+ hydrocarbons quantitation utilizing a FID and positive identification by a MS. GC2 utilizes a Dean switch with three columns: Quantitation of the low molecular weight hydrocarbon gases (e.g. methane and ethylene) is performed using an FID, and carbon dioxide (CO_2) and carbon monoxide (CO) are quantitated using two separate TCDs. The low molecular weight gases are separated on a Restek Rt-Alumina BOND 30 m x 0.32 µm x 5 µm column, while CO_2 is quantitated on a Restek Rt-QPLOT 50m x 0.32 µm x 5 µm column, and CO is quantitated on a Restek Rt Mol Sieve 30 m x 0.53 µm x 50 µm column. GC1 is calibrated using *n*-heptane as a standard and species were quantitated using the effective carbon number (ECN) method based on *n*-heptane response [44]. GC2 is calibrated with standard gas mixtures of known concentration prepared in helium purchased from Matheson Gas as shown in Table S1 of the Supplemental Material. CO and CO_2 were calibrated utilizing a separate mixture at 5000 ppm concentration in nitrogen (Matheson Gas). Measurement uncertainties are assumed to be about 15% for GC1, which is due to the use of the ECN method, variations in the sample delivery/sampling system, as well as the relatively higher molecular weight species measured in this system. GC2 quantitates lower molecular weight species which are easier to evaporate and have direct calibration standards and the associated uncertainty is assumed to be 10%.

2.2. Université de Lille (ULille) RCM

The ULille RCM was used to measure the ignition delay times (IDTs) of all three isomers and sample the reactants and intermediates during the ignition delay period. The driving piston is run by compressed air, which is mechanically engaged to the driven piston with a right-angle design metallic cam element to permit a repeatable compression phase. The grooved section at the end of the cam element holds the driven piston still at the end of the compression stroke to prevent piston rebound and keep the combustion chamber volume constant. The formation of a roll-up vortex from the thermal boundary layer during the compression stroke, which could eventually result in a considerable temperature field inhomogeneity [45], is prevented by using a creviced piston [46] and keeping the compression time

around 45 ms [47,48]. The combustion chamber has a bore of 50 mm and a stroke of 200 mm, and the compression ratio was set to 10.27. This cylindrical chamber is preheated by electric band heating elements with a maximum temperature deviation of 1 K along the axial direction. The pressure history throughout the experiment is acquired by a thermal shock-protected Kistler 6052CA31 piezoelectric transducer and a Kistler 5018 charge amplifier at 25 kHz signal sampling frequency.

The reactant mixtures were prepared in glass vessels by using the partial pressure method. Chemical products were purchased from Sigma-Aldrich with purities superior or equal to 98% (2M1B) or 95% (2M2B and 3M1B). Since 2M1B and 2M2B are in liquid phase at standard room temperature, they were conditioned by repeated freeze-thaw purification cycles to remove any eventual dissolved gases before the preparation of mixtures. This purification process of the fuel was unnecessary with 3M1B since this product was provided as a liquefied gas. N_2, O_2, and Ar were over 99.99% purity and supplied by Air Liquide. The initial temperature of the combustion chamber was fixed to 60±2 °C. The post-compression core gas temperature T_c was evaluated from the exact initial temperature, initial and compressed pressures assuming an adiabatic core and varied by using different inert gas compositions as provided in Table 1, while their inert-to-oxygen ratio was maintained at 3.76:1. T_c varies slightly for the different isomers, as their specific heat ratios are not completely identical to one another. Additional experiments, where O_2 was replaced by N_2, were performed to extract the volume histories used in the modeling of the experimental results [49], and are available as supplemental material. Representative pressure profiles for this study are pictured in Fig. 6a.

Table 1. Mixture mole fractions prepared for ULille RCM.

x_{C5H10}	x_{O2}	x_{N2}	x_{Ar}	$T_{c,\,avg}$ [K]
0.02725	0.2044	0.7684	0	700
		0.6916	0.07684	713
		0.6147	0.1537	728
		0.5379	0.2305	743
		0.4610	0.3074	759
		0.3842	0.3842	776
		0.2920	0.4764	798
		0.2075	0.5609	820
		0.1306	0.6378	842
		0.06916	0.6992	862
		0	0.7684	888

Sampling experiments are conducted by trapping the compressed mixture within a sampling canister through a sudden expansion at a desired time during the ignition delay period. The reactivity is frozen during the expansion process thanks to a volumetric ratio superior to 40 to 1, as demonstrated before [34,50]. Stable intermediate species formed during the ignition delay period are then identified and quantified by a Bruker Scion gas chromatography/mass spectroscopy (GC/MS) analyzing bench, in which the mixture is sent after separation by a Restek RT-QBond to two separate detection lines: A Mass spectrometer dedicated to identification of the intermediates, and a thermal conductivity detector (TCD)

- flame ionization detector (FID) line for quantification. Calibration was performed using in-house prepared mixtures for the fuels, and the ECN method for the quantified intermediates. An uncertainty on the reported selectivities of about 15% is assumed and is mostly due to the use of the ECN method, the complexity of the sampling, and the typical uncertainty of GC systems.

2.3. Argonne National Laboratory (ANL) RCM

ANL's twin-piston RCM (tpRCM) was utilized to acquire autoignition data for 2M2B. A detailed overview of the configuration as well as uncertainties associated with experimental measurements can be found in [51]. A brief overview is presented here. The tpRCM is pneumatically-driven and hydraulically controlled, using two opposed pistons to create the compression process. A ring-groove arrangement in the hydraulic chambers is used at the end of the stroke to facilitate deceleration, while the hydraulic chambers are pressurized during the test period to minimize piston rebound at ignition. The reaction chamber has a 50.8 mm bore with a nominal clearance height at maximum compression of ~25.5 mm; the volumetric compression ratio is near 12.1:1. The reaction chamber pistons incorporate crevices machined around their circumference to suppress vorticular motion during, and post-compression [47], as with the ULille RCM. The robustness of the configuration for the current study was verified, as demonstrated by Bourgeois et al. [52].

The exterior of the reaction chamber is heated using a combination of band, tape, and cartridge heaters, with high density insulation fitted between the flanges of the cylinders and the hydraulic chamber. Thermal uniformity of ±0.2% is achieved in the axial and azimuthal directions across the interior and exterior surfaces. The initial temperature of the chamber is varied from 30 to 85°C, with two different diluent gas blends to cover a range of compressed core gas temperatures, which is slightly different than the ULille technique. The dynamic pressure is measured using a Kistler 6045A-U20 transducer, regularly calibrated to 250 bar, and coupled to a Kistler 5064 charge amplifier. The 6045A-U20 is designed for thermal shock resistance ($\Delta P_{max} \leq \pm 1\%$) and incorporates a reinforced diaphragm for knock protection. The signal is recorded with a NI 9239 (24-bit/50kHz) data acquisition card, with the Savitzky-Golay algorithm applied to condition the record using a second-order fit in a filtering window of 0.25 ms.

Estimates of uncertainty and statistical (i.e., month-to-month) variations in the measurements are about ± 10% for ignition time. The non-reactive tests are also used to derive effective volume-time histories for chemical kinetic modeling where the rates of compression heating and pressure/temperature decay due to heat loss during the induction period can be reasonably taken into account [49]. The obtained volume-time histories are included in the supplemental material.

As with the ULille RCM, the post-compression core gas temperature T_c was evaluated assuming an adiabatic core. An uncertainty analysis associated with ANL's tpRCM is documented in [51], leading to $\pm 1.0\%$ in conservative estimate to T_c.

A 5.6-L stainless steel tank, heated to ~70°C, is used to prepare the fuel, diluent (Ar and N_2), and O_2 mixtures at different equivalence ratios. Liquid 2M2B (≥99% purity) at room temperature is first injected into the evacuated tank through a septum, and then the high purity gases are supplied in the sequence of Ar (99.9997%, Airgas), N_2 (99.9998%, Airgas), and O_2 (99.9997%, Airgas). No freeze-thaw purification

was performed for the 2M2B used in these tests. However, the effect of eventual dissolved gases is expected to be minimized when the fuel is injected from a syringe directly into the tank, in comparison with the evaporation technique used in ULille. After blending the constituents, the mixture is allowed to diffusively mix for a minimum of 45 minutes before beginning the tests. The evaporation efficiency of each test fuel is calculated from ideal gas relationships, with ~95% typically achieved, while the mass of fuel and partial pressure of gaseous components are used to determine the molar composition of the mixture. Detailed mixture compositions are provided in Table 2.

Table 2. Mixture mole fractions prepared for tpRCM. Note that these mixtures are in diluted condition, compared to standard air composition.

Equivalence ratio	x_{2M2B}	x_{O2}	x_{N2}	x_{Ar}
0.5	0.00825	0.12375	0.86800	0
	0.00823	0.12373	0.43429	0.43375
1.0	0.01634	0.12254	0.86112	0
	0.01637	0.12259	0.42954	0.43150
2.0	0.03218	0.12083	0.84699	0
	0.03219	0.12067	0.42259	0.42455

3 Kinetic modeling

The kinetic model developed in the present work is based on the high temperature modeling work of [16] for 2M2B, [18] for 3M1B and [53] for 2M1B. The reaction classes relevant to alkene oxidation, as previously identified [15,25] have been implemented to build a consistent kinetic model of the three methylbutene isomers at low-to-intermediate temperature conditions. These different classes, as well as the origin of the used rate coefficients, are detailed below.

3.1. Radical Addition reactions

It has been demonstrated in previous studies that radical addition reactions to the double bond constitute an important contribution to the reactivity of alkenes in the low-temperature region [9,15]. The accurate description of these pathways can also play an important role in the prediction of the reactivity at all temperatures. The addition of an OH radical to the double bond in propene has been studied theoretically by Zádor et al. [54] and their calculations were adopted for analogous addition reactions of the methyl butenes in this study. At low temperatures, the primary product expected from the alkene+OH reaction is an hydroxyalkyl radical which will typically be followed by addition of O_2. For a long time, this $HORO_2$ radical has been understood to undergo Waddington decomposition [41]. This proceeds through intramolecular H-transfer from OH to the peroxy moiety followed by rapid decomposition producing two carbonyl molecules and an OH radical, thereby constituting a chain-propagating reaction sequence. Recent theoretical works [55] have shown that $HORO_2$ radicals could participate in pathways, classified as alternative-Waddington pathways, depending on the structure of the parent molecules. These alternative-Waddington pathways proceed through intramolecular H-transfer reactions producing OHQOOH radicals, in a similar fashion to RO_2 to QOOH isomerizations which are typically observed for alkanes. OHQOOH radicals could participate in many of reactions which include unimolecular decompositions, second O_2 additions and formation of hydroxy-cyclic ethers. All

these reaction classes have been considered in the present mechanism using analogous reaction rate parameters from [55]. These alternative-Waddington pathways have been found to be considerably active in determining the reactivity of linear pentenes [56] and di-isobutylene isomers [33].

At low to intermediate temperatures and pressures over one atmosphere, HO_2 addition to the double bond will typically yield a QOOH radical, an epoxide+OH, or a peroxy radical as discussed in [37]. The specific QOOH and RO_2 radical isomers formed are dependent on the carbon atom in the double bond with which the HO_2 radical reacts. The QOOH radical can also subsequently undergo a unimolecular reaction forming an epoxide+OH, thereby converting a relatively unreactive HO_2 radical into a reactive OH radical. At very low temperatures, the addition of HO_2 to an alkene results in an RO_2 radical [37]. All three potential product channels (QOOH, epoxide+OH, RO2) relatively enhance the reactivity of the methyl butene isomers in the low to intermediate temperature range and the hydrocarbon products correspond to intermediates in the submechanism for isopentane [57]. O-atom addition reactions to the double bond were also included by adopting analogous reactions based on calculations by Cavallotti et al. [58]. Furthermore, the reactions and the associated rate parameters related to H-radical addition to methyl-butene isomers have been updated in the present mechanism using the kinetics from a recent ab-initio study of Power et al. [59]. This PES modelled in the mechanism included formation of iso-pentyl radicals, and the chemically activated pathways. These chemically activated pathways include formation of pentyl isomers and β–scission pathways producing smaller fragments (C_1-C_4).

3.2. H-abstraction reactions

2M1B and 3M1B possess alkylic, allylic, and vinylic carbon atoms while 2M2B has only allylic and vinylic carbon atoms. All H-atom abstraction reaction rate parameters were calculated by Power et al. [59] and adopted in this work. The H-atom abstractions by O_2, O, OH, HO_2, CH_3 and CH_3O_2 at alkylic positions are taken similar to alkanes in [60]. At allylic positions, the H-atom abstractions reaction rate parameters are estimated on the basis of propene or but-1-ene. For the three isomers, three different allylic carbon sites are considered: primary allylic (PA), secondary allylic (SA) and tertiary allylic (TA). The PA and SA sites are estimated by similarity to propene and but-1-ene considering the H-atom abstractions by O_2 [61], by OH [54,62], by HO_2 [37], by O, CH_3, CH_3O and CH_3O_2 [60]. The H-atom abstraction reactions at a TA site are taken in analogy with but-1-ene but with 1 kcal/mol reduction on the activation energy to consider the difference in the bond dissociation energy in C-H for a secondary and tertiary site. The H-atom abstraction reaction rates at vinylic carbon sites by H, O, OH, HO_2, O_2 and CH_3 are taken similar as propene from the work of Burke et al. [63].

3.3. Further reactivity of allylic radicals

Allylic radicals are formed by H-atom abstraction from methylbutenes and their subsequent reactions are described in the kinetic model. The reactions of allylic radicals considered include reactions with O_2, HO_2, self-recombination reactions, and recombination reactions with methyl-radicals.

Addition of allylic radicals to O_2 lead to the formation of allylic peroxy adducts. The well-depths for addition of O_2 allylic radicals are shallower (~ 20-24 kcal/mole) compared to that of alkyl-peroxy adducts and for a long time these adducts have not been included in kinetic mechanisms. However, our recent mechanisms for iso-butene [10] and di-isobutylene [33] have shown that allylic-peroxy adducts could

have a considerable effect on the reactivity of olefins. For this reason, we have added these reaction classes into our mechanism using the kinetics from Chen and Bozzelli [64]. These reactions, in the case of methylbutenes isomers, facilitate the formation of isoprene (B13DE2M), unsaturated aldehydes or unsaturated ketones. Additionally, the kinetic model recently published by Grajales-Gonzalez et al.[65] for the pyrolysis of isoprene was included in the present model.

The addition of an HO_2 radical at an allylic site can form an unsaturated hydroperoxide at low temperatures. This unsaturated hydroperoxide will decompose to an alkenoxy radical and an OH radical. At higher temperatures, this unsaturated hydroperoxide adduct becomes thermally unstable and the R+HO_2 reaction proceeds via well-skipping to the alkenoxy radical and an OH radical. Rate coefficients for HO_2 addition to allylic radicals were adopted based on analogy to the allyl+HO_2 reactions from Goldsmith et al. [66] [67]. Finally, the addition of oxygen atoms to the allylic radicals were modelled using benzyl + O analogies from the study of da Silva and Bozzelli [68].

H-shift isomerizations [69] and β-scissions [60] are significant pathways in the high temperature chemistry of isopentenyl radicals. The self-recombination reactions of allylic C_5H_9 radicals were also considered and the kinetic parameters are estimated to be the same as allyl recombination [70]. The reactions of allylic C_5H_9 with methyl-radicals have also been considered and have been modelled using analogies from iso-butene chemistry.

3.4. Further reactivity of vinylic radicals

Because of the high bond dissociation energy of vinylic C-H and C-C bonds compared to allylic bonds, the formation of vinylic methylbutenyl radicals only becomes of some importance at higher temperatures. The reactions of such radicals with O_2 were adopted using analogous reactions from [71].

3.5. Reactivity of alkylic radicals

As in the case of allylic radicals, the unimolecular pathways for alkylic methylbutenyl radicals were included based on the calculations by [72]. The pathways following O_2 addition, which include RO_2 to QOOH isomerization pathways were included following rate coefficient suggestions by [40]. These isomerizations are favored by the presence of allylic sites, which has a strong influence on the formed products. Using the CBS-QB3 method, You et al. [40] explored the potential energy surface of the alkenylperoxy radicals and computed reaction rate constants using canonical/variational transition state theories. Interestingly they found that RO_2 intramolecular ring closure reactions show a lower energy barrier in comparison to internal H-atom migration reactions or concerted HO_2 elimination reactions. The corresponding pathways for the alkylic radicals formed by 2M1B and 3M1B are illustrated in Fig. 2.

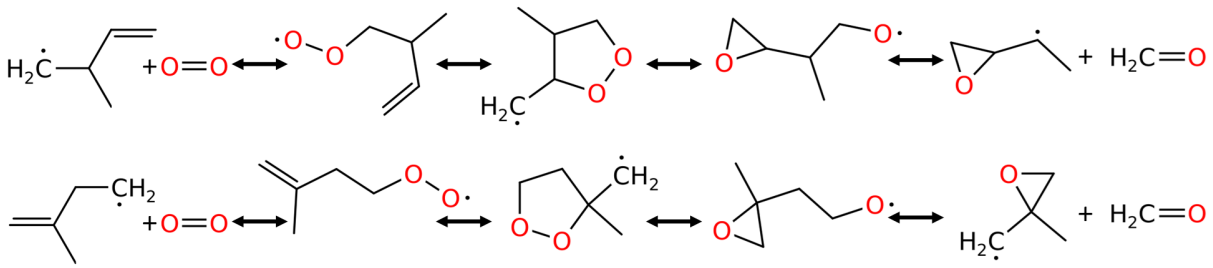

Figure 2: Favored reaction pathway of alkyl radicals + O_2 through intramolecular addition reactions

After the intramolecular ring closure of the alkylic RO_2, the resultant radical may proceed through a unimolecular reaction producing an alkoxy epoxide radical. The β-scission of this alkoxy epoxide radical produces formaldehyde and alkyl epoxide radical. Due to the relatively low energy barrier of the RO_2 intramolecular ring closure, these reactions can play a role in the reaction kinetics of the alkylic methylbutenyl radicals and are included in the current kinetic model.

4. Results and discussion

4.1. Speciation from the NREL flow reactor

Mole fractions of the several intermediate species at intermediate temperatures were measured at the outlet of a flow reactor in NREL and are compared with simulation results in Figs. 3-5. The simulations were performed using Cantera [73] as a plug flow reactor, which was modeled as a linear chain of zero-dimensional reactors. The composition of the first reactor was specified as the initial mixture composition (of the experiments) and for the succeeding reactors the inlet composition was the outlet composition of the reactor upstream. The individual zero-dimensional reactor temperatures were set based on the temperature profiles of the flow reactor provided in the Supplemental Material. All three isomers share a common pathway which leads to the production of isoprene in significant amounts as reported by Arafin *et. al.* in shock tube experiments [20]. In the case of 2M1B, the conversion of the fuel is observed at temperatures above 950 K and increases with temperature until all fuel is converted at a temperature of about 1080 K. The observed conversion is accurately reproduced by the model as seen by the predicted 2M1B profile shown in Fig. 3. Conversion of the fuel yields significant amounts of methane, isoprene, and CO, all of them being well captured in the simulations. At lower reactor temperatures, the initial formation of propyne is observed and well captured, but propyne is overpredicted by a factor of 3 at higher temperatures. Traces of soot pre-cursor components (cyclopentadiene) and aromatic compounds were also measured; the most abundant being benzene, followed by toluene, ethylbenzene, and xylene. The model agreement on these species is fair, with the modeled mole fraction of benzene being underestimated by the model by about a factor of two.

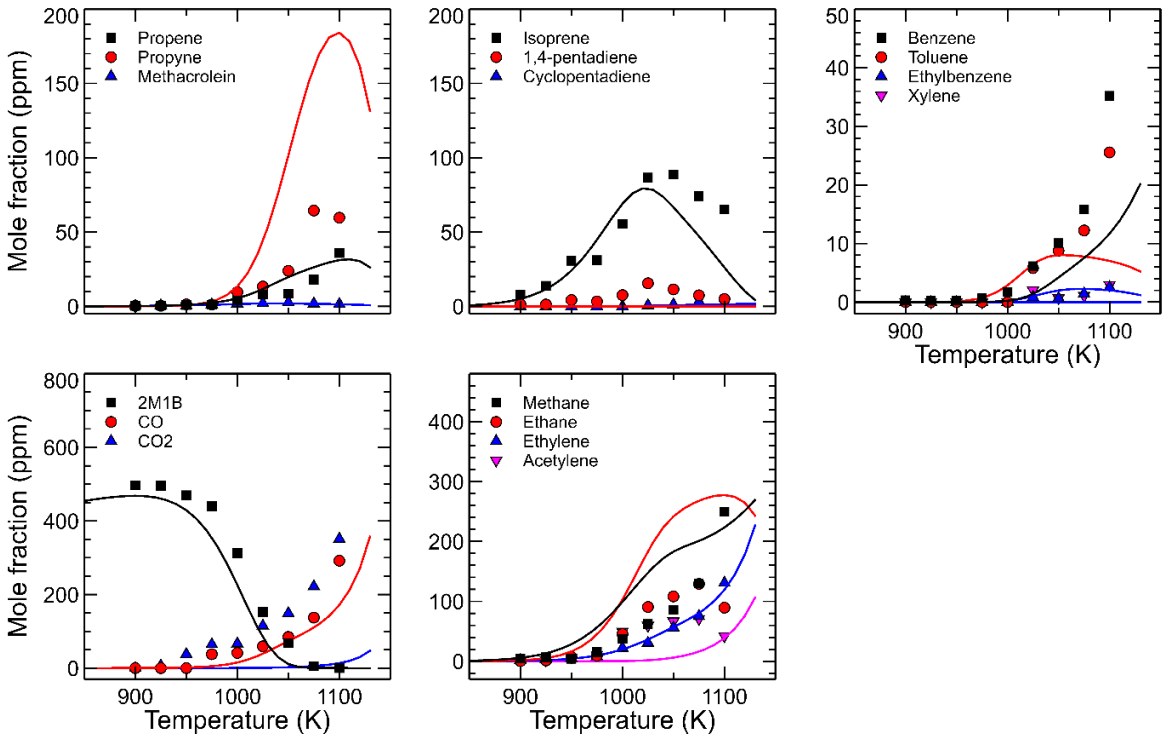

Figure 3: Comparison of experimental (symbols) and simulated (lines) mole fraction-temperature profiles obtained in the NREL flow reactor during the oxidation of 2M1B. ϕ = 1.0, δ = 0.35 s.

The comparison of experimental and simulated mole fraction-temperature profiles during the oxidation of 2M2B shows that the conversion of this isomer begins at temperatures greater than 980 K, with the fuel being fully converted at about 1120 K, as can be seen in Fig. 4. This is the slowest reacting isomer of the three, with complete conversion occurring 40 K higher than for 2M1B and almost 100 K higher than for 3M1B (Fig. 5). The model predicts the fuel conversion, isoprene, propene, methane and CO with good accuracy. Similar to the case of 2M1B oxidation, propyne is underpredicted by the model by a factor of two. In addition, the formation of aromatic species from this isomer was not experimentally observed in appreciable amounts, in contrast to the 2M1B isomer (Fig. 3).

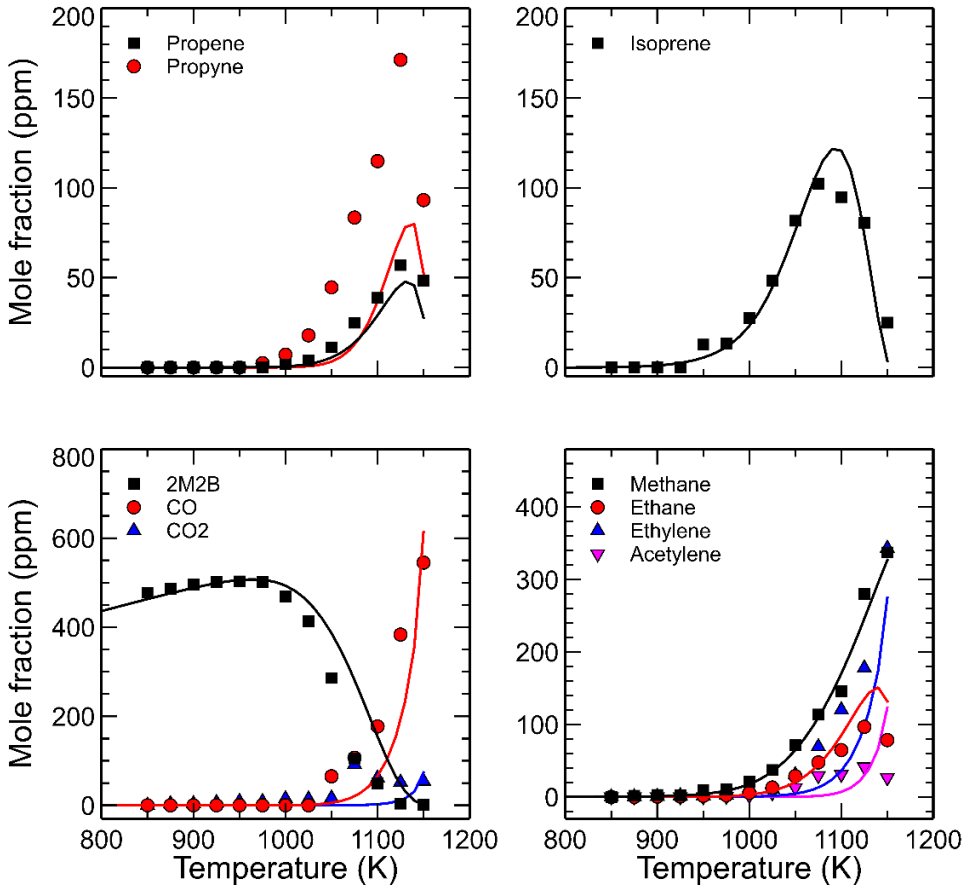

Figure 4: Comparison of experimental (symbols) and simulated (lines) mole fraction-temperature profiles obtained in the NREL flow reactor during the oxidation of 2M2B. ϕ = 1, δ = 0.35 s.

The comparison of the experimental and simulation data for 3M1B is displayed in Fig. 5. The conversion of the fuel starts at temperatures above 900 K, the lowest starting temperature in comparison with the other two isomers. Measured fuel consumption in the flow reactor occurs at temperatures lower by about 25 K than predicted by the model. CO, butadiene, propene, ethylene, and ethane are the products formed in the highest quantities. Predictions of propene and 1,3-butadiene are initially well captured by the model, but then are over-predicted by almost a factor of two at higher temperatures (i.e., above 1000 K). Isoprene, CO, CO_2, methane, and ethylene are all observed experimentally well before model predictions, though the general trend is captured by the model. In contrast, ethane is

predicted to form in concentrations two times higher than what was observed experimentally. As with 2M2B, there are no aromatic species produced in measurable amounts from this isomer.

The model is best able to capture the reactivity and formation of intermediate species for the 2M1B and 2M2B isomers, however the formation of CO_2 and aromatic species are underpredicted in the case of 2M1B (Fig. 3). 3M1B is observed to be completely consumed experimentally about 25 K lower in temperature than what is predicted by the model. In addition, several species are observed experimentally well before model predictions for both 3M1B, which is especially true in the case of isoprene and CO.

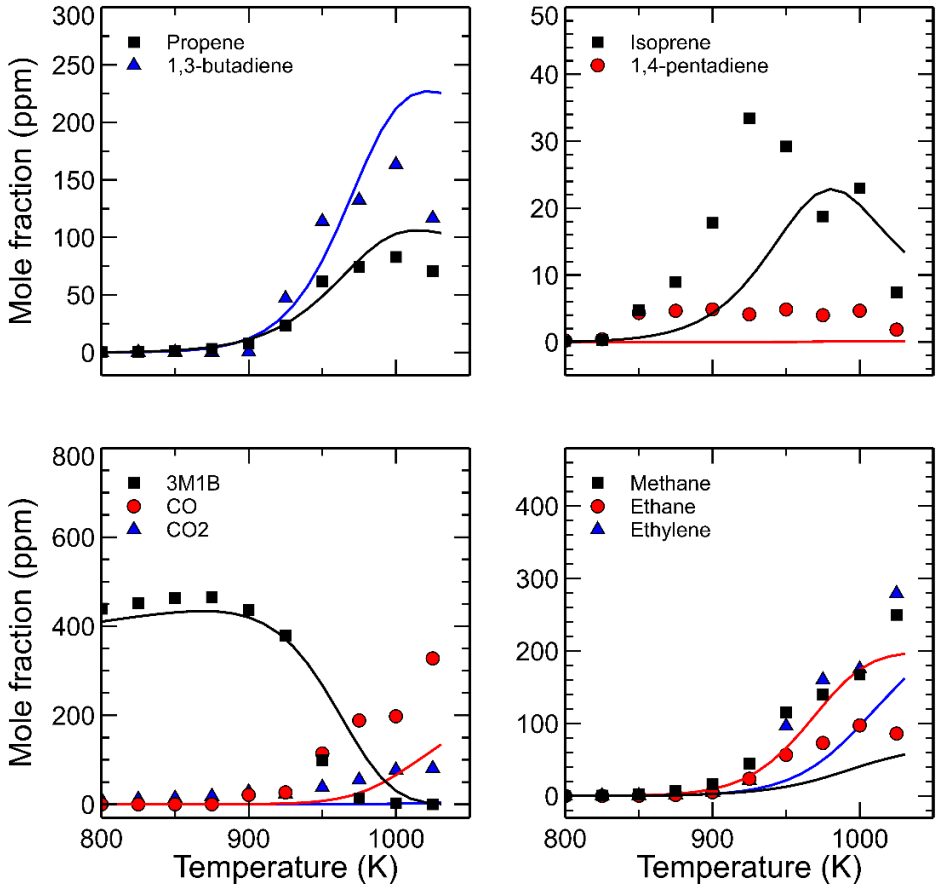

Figure 5: Comparison of experimental (symbols) and simulated (lines) mole fraction-temperature profiles obtained in the NREL flow reactor during the oxidation of 3M1B. ϕ = 1, δ = 0.35 s.

4.2. Measured and computed IDTs

The IDT in this study is defined as the elapsed time from the end of the compression (denoted EOC), until the moment where maximum pressure rise rate occurs for both the experimental results and the simulations. The RCM simulations were conducted using the Zero-RK solvers [74]. Figure 6 depicts representative pressure profiles acquired from the ULille RCM and the ANL tpRCM for reacting and non-

reacting experiments. Note that there are at least two experimental pressure records provided for each test point, demonstrating excellent shot-to-shot repeatability for both RCMs used in this study.

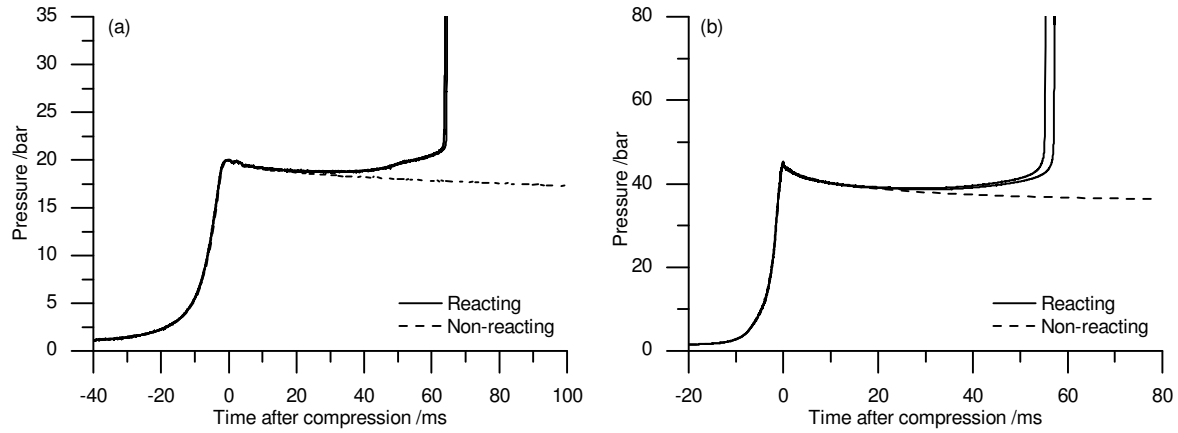

Figure 6.: Representative pressure profiles of (a) 2M1B in ULille RCM at T_C = 700 K, P_C = 20 bar, equivalence ratio ϕ = 1.0 for three repeated test shots and (b) 2M2B in ANL tpRCM at T_C = 729 K, P_C = 45 bar, ϕ = 1.0 in diluted condition for two repeated test shots.

Comparison of reacting and non-reacting pressure profiles shows significant exothermicity before ignition, as already observed for a number of hydrocarbons including alkenes [9,75], in the diluted as well as the non-diluted conditions. In the case of 2M1B and 3M1B, the pressure profiles at the lowest temperatures are reminiscent of two-stage ignition, though the extent of the first stage is so faint that it does not allow the precise measurement of first-stage ignition delays from the pressure profiles. These observations correspond well with a recent 2M2B study [16], in which the authors reported no evidence of low-temperature reactivity.

IDTs of all three isomers were obtained from the ULille RCM at 700–890 K core gas temperatures under 10–20 bar EOC pressure conditions and an equivalence ratio of ϕ = 1.0, while the ANL tpRCM work focused on diluted 2M2B mixtures at equivalence ratios of ϕ = 0.5, 1.0, and 2.0, compressed temperatures between 685–1020 K and two EOC pressures of 25 and 45 bar. The ULille experimental IDT measurements are shown in Fig. 7 along with the simulation results. A slight deviation from Arrhenius behavior is clearly observed for 2M1B and 2M2B, this deviation being significant in the case of 3M1B. The model predicts the ignition delays fairly, the agreement being within a factor of two in the worst case, i.e., for 2M1B and 2M2B for the highest pressures. A comparison of the three isomers, as pictured in Fig. 7d, shows that 3M1B, despite demonstrating significant non-Arrhenius behavior, has the longest ignition delay at all temperatures accessed in this study. 2M1B shows the shortest ignition delays at the lowest investigated temperatures, while 2M2B is the most reactive at the highest temperatures. The simulations adequately reproduce these trends but predict longer ignition delays than the experiments for 2M1B and 3M1B at the highest investigated temperatures.

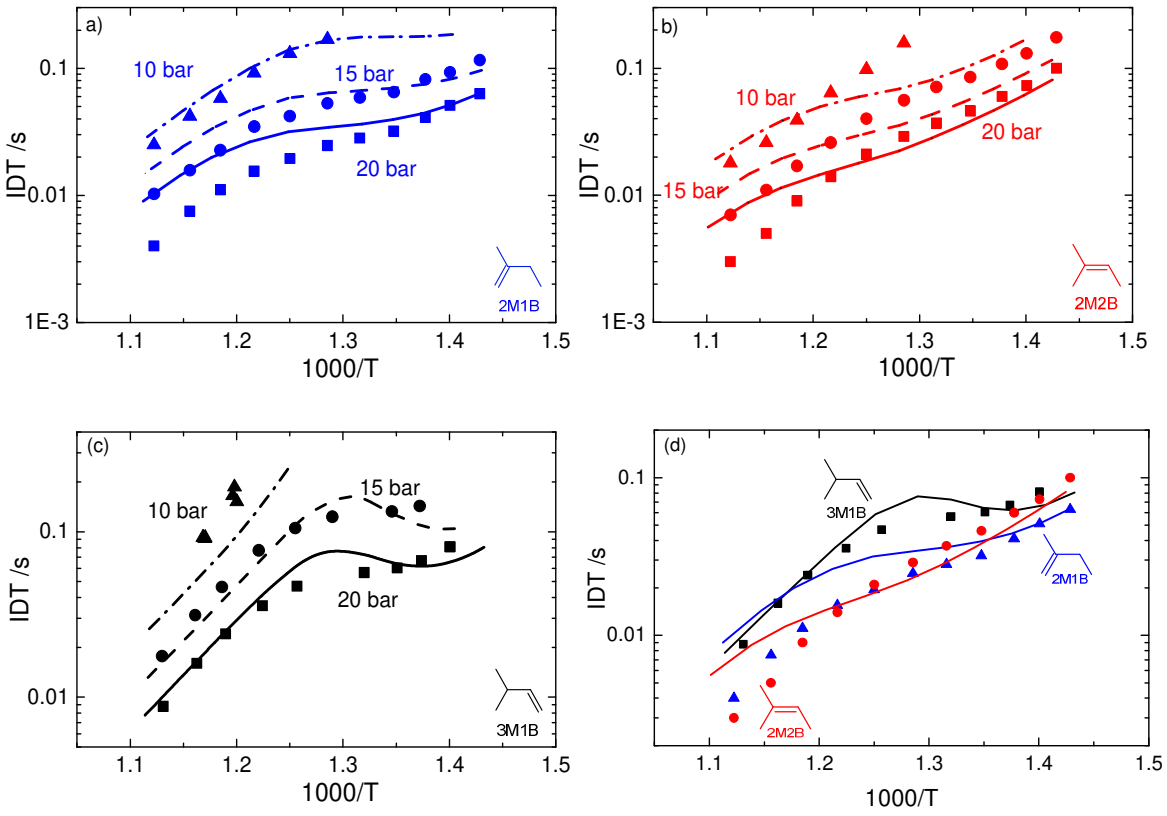

Figure 7. Ignition delay times of the methylbutene isomers. (a) 2M1B, (b) 2M2B, and (c) 3M1B from ULille RCM. (d) Comparison of the three isomers for the p_C = 20 bar condition. ϕ = 1.0, inert/O_2 = 3.76.

The ANL tpRCM results for diluted 2M2B are shown in Fig. 8. In this case, the deviation from Arrhenius behavior is mostly visible at the fuel-rich condition but is not as pronounced as for the other isomers. The agreement between the experiments and the simulation is also good in this case, with the maximum deviation observable for fuel-rich conditions at high temperatures.

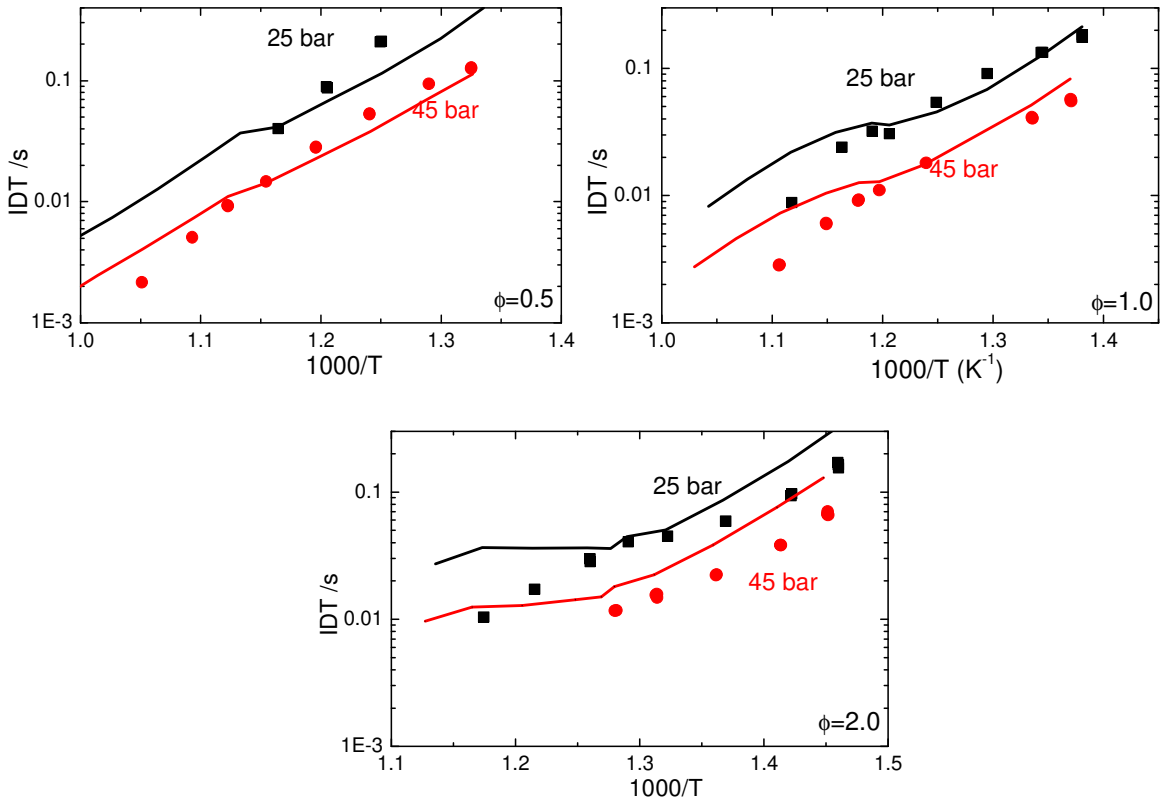

Figure 8: Ignition delays of 2M2B under diluted conditions, at different equivalence ratios from ANL tpRCM. inert/O_2 = 7.

4.3. Speciation from the ULille RCM

Dozens of stable intermediate species were identified from the mixture sampling experiments of the three methylbutene isomers during the ignition delay period at 730±1 K and 20±0.2 bar condition. The moment of sampling was fixed between 0.85–0.92 of the normalized IDTs of each isomer, where a value of one corresponds to ignition and a value of zero corresponds to end of compression. At the sampled times of this study, the fuel conversion was about 17.9% (2M1B), 19.5% (2M2B), and 14.1% (3M1B). It is notable that some intermediate species are common between these isomers, mostly because of the formation of resonance stabilized allylic radicals after the first H abstraction, were some of the radicals are common to several isomers. For example, the 2-methyl-2-buten-4-yl radical from 2M2B and the 3-methyl-1-buten-3-yl radical from 3M1B are both the same resonance stabilized radical. Hence any intermediate spawning from these radicals can be observed for both fuels.

From the measured mole fractions, the results are reported as selectivities, which are expressed as:

$$s_i = \frac{x_i}{\sum_{i=1}^{N} x_i}$$

where s_i is the selectivity of *i*-th species, x_i is the mole fraction of *i*-th species, and N is the number of the identified oxidation products from the GC. The use of selectivities enables comparing the relative formation of the intermediate species. It also allows the potential dilution effect of the gases trapped in the crevice, which will also be unavoidably sampled, to be neglected.

Experimental selectivities of the stable intermediate species from all the isomers are compared with the simulation results in Fig. 9 and provided as a table in the supplemental material. 2M1B and 2M2B were present as impurities in the 3M1B fuel, with mole fractions between 1.5 and 2%. This resulted in high measured experimental selectivities, mostly because of the low observed conversion of 3M1B. As a consequence, the selectivities of these products are not reported.

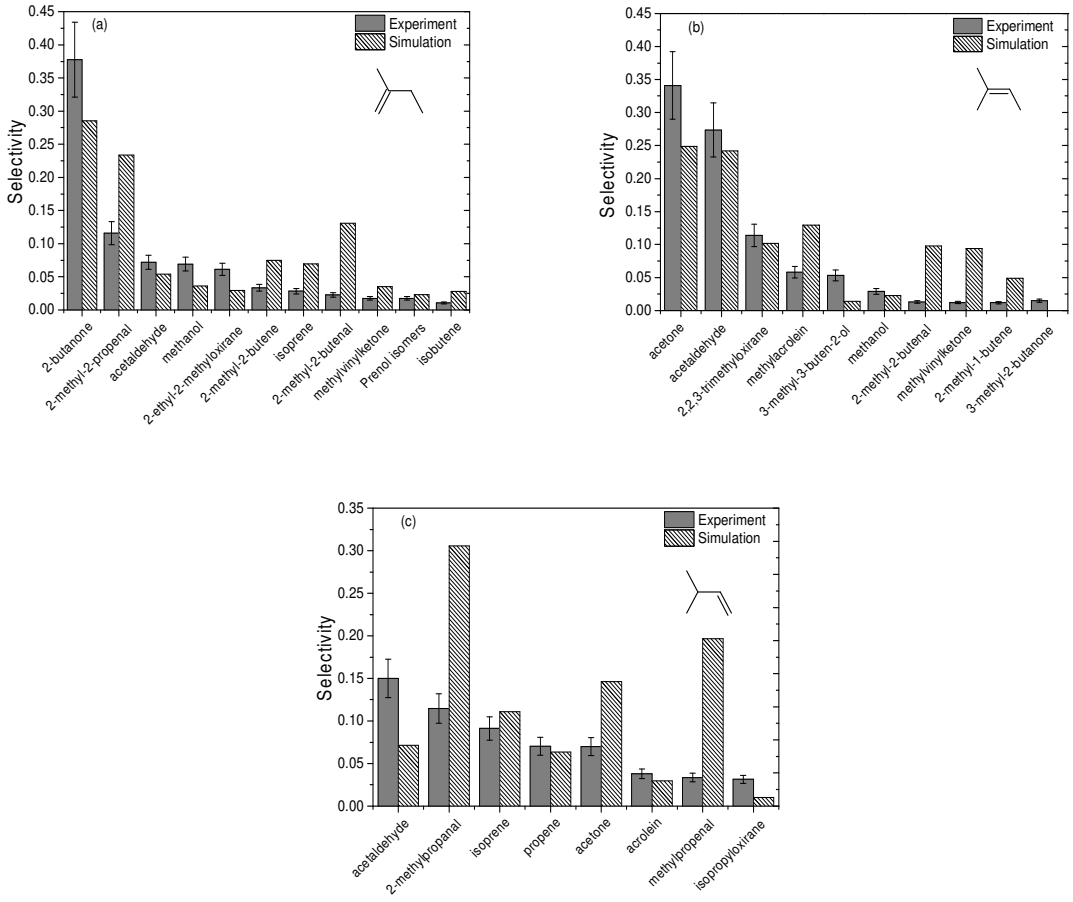

Figure 9: Measured and simulated selectivities of the main intermediates formed during the ignition delay of the methylbutene isomers in ULille RCM, at a normalized time of t/τ between 0.85–0.92 (see text). T_C = 730 K , Pc = 20 bar, undiluted ϕ = 1.0

The simulated selectivities were inferred at the same t/τ as in the experiments. The IDTs between the experiments and simulations agree within 20% at these conditions for all isomers. This gives some confidence that the experimental and simulated selectivities are compared at approximately the same time with regards to the global reactivity of the mixture. The agreement in the selectivities is within 30%

on the Waddington products, as witnessed by the measured and simulated mole selectivities of 2-butanone for 2M1B, acetaldehyde and acetone for 2M2B, a notable exception being 2-methylpropanal for 3M1B which is overestimated by about a factor of three. The formation of oxiranes by HO_2 addition to the double bond is underestimated for 2M1B (2-ethyl-2-methyloxirane) and 3M1B (isopropyloxirane), respectively, but accurately predicted in the case of 2M2B (2,2,3-trimethyloxirane). On the other hand, products spanning from the reactivity of allylic radicals by addition to O_2 or with HO_2 appear to be overestimated by the model, as demonstrated by comparing the experimental and simulated selectivities for 2-methyl-2-butenal for all isomers.

In addition to the newly obtained data, the kinetic model has also been used to model laminar burning velocity data [76] and jet-stirred reactor data [16] from the literature, showing very good agreement on the former and good agreement on the latter, as demonstrated in the Supplementary Material.

4.4 Rate of Production analysis

To shed further light on the dominant pathways as predicted by the kinetic model, rate of production analyses were performed in the conditions of the RCM sampling experiments, and are displayed in Fig. 10. In these conditions, the dominant pathway is the formation of allylic radicals, representing 45% of the conversion of 2M2B, and 39% for 2M1B and 26% for 3M1B. Note that the allylic radicals each have two resonant structures which lead to different isomer products, but only one of resonant structures is displayed in Fig. 10. These allylic radicals mostly react with HO_2 radicals to form hydroperoxides, which will in turn yield methylbutenoxy and OH radicals. This pathway is however likely to be overestimated by the model, as visible from the large discrepancy on the 2-methyl-2-butenal selectivities discussed in the previous section. Allylic methylbutenyl radicals can also recombine to form dimers, that were detected experimentally in the ULille RCM but were not quantified because of their low signal. A small fraction of the allylic radicals also adds to O_2, essentially leading to the formation of isoprene along with an HO_2 radical. In the case of 2M1B and 3M1B, non-allylic radicals are also formed, for which the addition to O_2 is more preferential than for allylic radicals. One can however note that the formation of ketohydroperoxides is only non-trivial for the case of 3M1B, where it constitutes a minor pathway. Instead, cyclisation can take place on the vinylic site, leading to a C_4 alkenoxy radical and formaldehyde, as demonstrated for 2M1B and 3M1B and discussed in Section 3.5.

Addition of OH radicals to the double bond is also a major oxidation pathway for all three isomers at the conditions sampled, representing 25%, 29% and 40% of the conversion of 2M1B, 2M2B and 3M1B respectively. The resulting hydroxyalkyl radicals then mostly react with O_2 forming a $HORO_2$ species. The $HORO_2$ species can then undergo a Waddington decomposition to carbonyls + OH or an isomerization to a HOQOOH radical. HOQOOH radicals formed may enable a second O_2 addition reaction to occur and ultimately the formation of more than one OH radical, i.e. chain branching. These pathways resulting from OH addition are of importance to the accurate prediction of ignition as they will lead to the formation of one or more OH radicals. Intermediates definitively linked to these HOQOOH were however not observed experimentally, being too unstable to survive GC analysis.

Finally, the direct addition of HO_2 to the double bond can yield oxiranes, as discussed earlier. This is only predicted to correspond to 7% of the overall conversion of 2M2B, and less for the other isomers. This

echoes the discrepancy between the simulated and measured selectivities of oxiranes and calls for further investigation of this addition reaction.

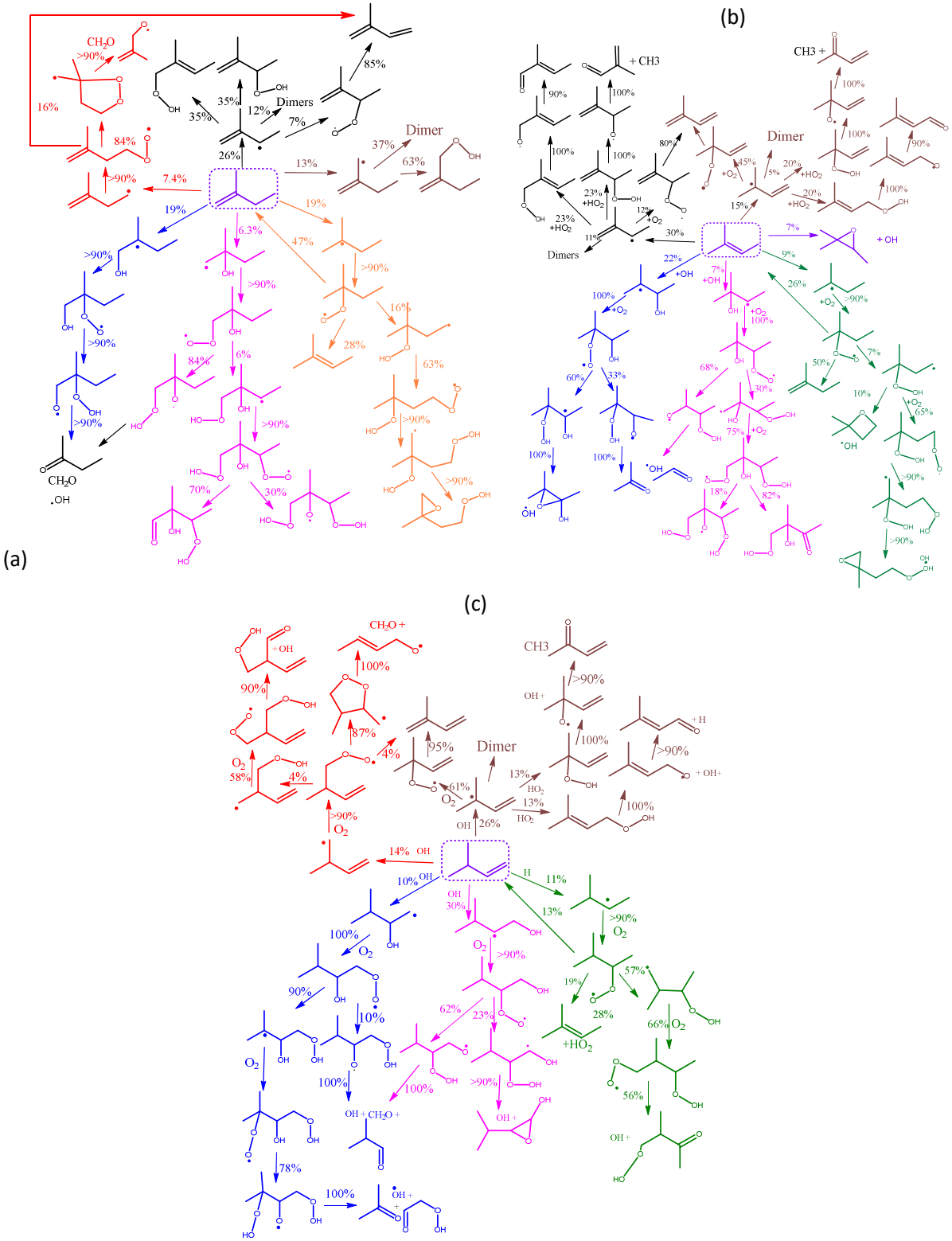

Figure 10: Rate of production analyses performed for 2M1B (a), 2M2B (b), and 3M1B (c) in ignition delay conditions. T_C = 730 K, Pc = 20 bar, undiluted ϕ = 1.0.

4.5 Sensitivity analysis

Brute-force sensitivity analyses were performed on the ignition delay at 730 K and 20 bar in the undiluted, stoichiometric RCM conditions. The results are shown in Fig. 11 for all three isomers. Many reactions were included in this figure in order to allow gaining some insight from the comparison of relative sensitivities for the three isomers. The reactions were grouped in several classes to facilitate analysis and discussion.

One can note that for all three isomers at 730 K, the reaction contributing the most to a decrease of the ignition delay is the addition of the OH radical on the double bond. This is due to the potential for O_2 addition which can lead to a Waddington decomposition (chain propagating) or HOQOOH formation (chain propagating or chain branching), as discussed above and in [15]. The sensitivity coefficient of the addition of the OH radical on the double bond is however, far smaller at 900 K. The abstraction of a hydrogen atom by OH is, on the other hand, a significant contributor to a decrease of the ignition delay at 730K. The competition between both reactions on the OH radicals at 730 K has thus an important influence on the predictive ability of the model at 730 K. Further optimization of the branching between H-abstraction by OH and OH addition to the double bond, especially in the 2M1B case, could help improving the performance of the model on the prediction of the IDTs at the highest temperatures. However, any local optimizations of the site-specific H-atom abstraction rate constants should attempt to (1) minimize perturbations of the overall rate constant, (2) apply the locally optimized rate constant for a site as a rate rule to analogous reactions accordingly. In this case, the 2-methylbutenes share four analogous H-atom abstraction by OH reaction sites. Therefore, improving the simulations for one isomer via modification of H-atom abstraction by OH reactions may adversely affect another isomer. For the sake of the model's consistency, such an optimization was therefore not performed.

Another notable class of reactions is the formation of isoprene (noted B13DE2M) and HO_2 from the peroxyalkenyl radicals resulting from the addition of allylic methylbutenyl radicals to O_2. One can note that the sensitivity coefficient for this reaction is positive at 730 K, but negative at 900 K. This can be explained by the fact that isoprene is likely to show very limited reactivity towards ignition at 730 K, and that this reaction competes with other pathways of the peroxyalkenyl which would lead to the formation of OH radicals. Nonetheless, HO_2 radicals are important drivers of reactivity at 900 K since they can yield H_2O_2 which rapidly decomposes to two OH radicals. However, at 730 K, there is a competition between the reaction sequence leading to isoprene after addition to O_2 and the termination reaction between methylbutenyl and HO_2 radicals ultimately yielding OH radicals, this branching being of importance in the accurate prediction of the ignition delay.

The recombination reactions of allylic methylbutenyl radicals to form dimers are also of importance, especially for 2M1B and 2M2B, and decrease the global reactivity of the system by removing methylbutenyl radicals from the system. Their competition on these radicals with the additions to HO_2 radicals are also important in the accurate prediction of the ignition delays, the latter having negative sensitivity coefficients at both temperatures. Finally, the direct additions of HO_2 radicals to the double

bond are only significantly sensitive in the case of 2M2B and 3M1B, where it can contribute to a decrease of the ignition delay at 730 K by yielding an OH radical.

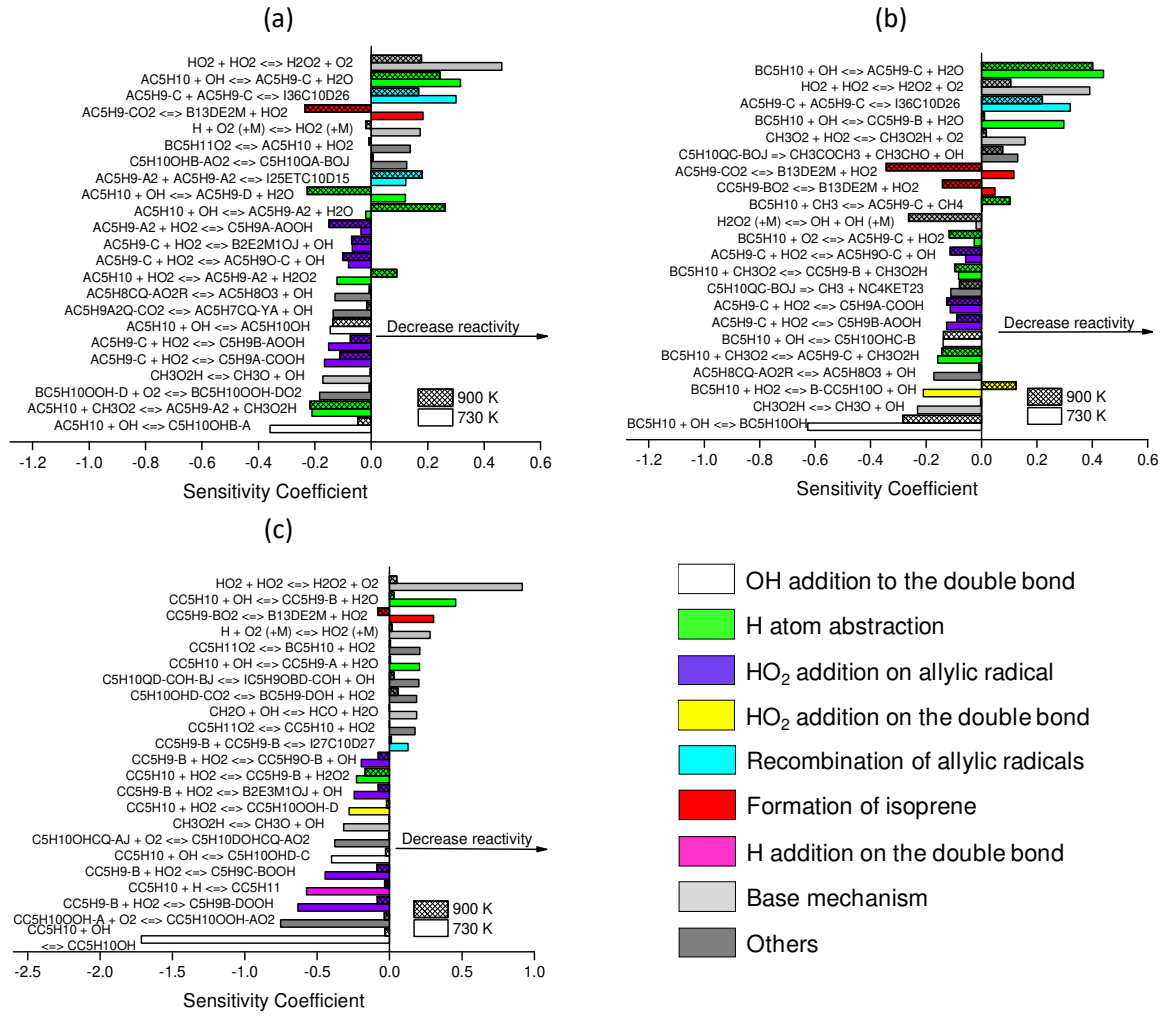

Figure 11: Brute-force sensitivity analyses on the ignition delay of 2M1B (a), 2M2B (b), 3M1B (c). T_C = 730 K , Pc = 20 bar, ϕ = 1.0.

5. Conclusions

A detailed experimental and kinetic modeling study has been performed for the three isomers of methylbutene, with help from new experimental data obtained in the NREL flow reactor, and the ANL and ULille RCMs. A kinetic model has been built with help from recent kinetic data, in a consistent way for all three isomers. It shows fair performance in predicting the newly obtained experimental data as well as Jet-Stirred Reactor and Laminar Burning Velocity data from the literature. The results suggest

that the reactivity of methylbutene isomers at low temperatures is governed by the competition towards OH radicals of the OH addition to the double bond and the H-atom abstraction, as well as a competition on HO_2 radicals of the formation of H_2O_2 and the addition of HO_2 on methylbutenyl radicals or on the double bond. It was observed experimentally that dimers of methylbutenyl radicals are formed, their formation reactions constituting sensitive reactions. This stresses the importance of including such reactions inside kinetic models describing the oxidation of large molecules that are able to form resonance-stabilized radicals. In the case of the three isomers the formation of isoprene is notably sensitive, suggesting that further investigation of the oxidation of that molecule would be beneficial to the improvement of the current model. Finally, the remaining discrepancy between the predictions and the measured selectivities of products formed in RCM conditions calls for additional work on the additions of HO_2 radicals to the double bond or to allylic radicals.

Acknowledgements

The work at LLNL was performed under the auspices of the U.S. Department of Energy (DOE) by Lawrence Livermore National Laboratory under Contract DE-AC52-07NA27344 and was conducted as part of the Co-Optimization of Fuels & Engines (Co-Optima) initiative sponsored by the DOE Office of Energy Efficiency and Renewable Energy (EERE), Bioenergy Technologies and Vehicle Technologies Offices. This research performed in ULille was funded by TOTAL Marketing Services and is a contribution to the CPER research project Climibio. HS and GV thank the Région Hauts-de-France, and the Ministère de l'Enseignement Supérieur et de la Recherche (CPER Climibio), and the European Fund for Regional Economic Development for their financial support.

References

[1] J.P. Szybist, D.A. Splitter, Understanding chemistry-specific fuel differences at a constant RON in a boosted SI engine, Fuel. 217 (2018) 370–381.

[2] K.P. Somers, R.F. Cracknell, H.J. Curran, A chemical kinetic interpretation of the octane appetite of modern gasoline engines, Proc. Combust. Inst. 37 (2019) 4857–4864.

[3] M. Kassai, C. Aksu, T. Shiraishi, R. Cracknell, M. Shibuya, Mechanism Analysis on the Effect of Fuel Properties on Knocking Performance at Boosted Conditions, in: SAE Technical Paper 2019-01-0035, 2019.

[4] G.T. Kalghatgi, Fuel Anti-Knock Quality - Part I. Engine Studies, in: SAE Technical Paper 2001-01-3584, 2001.

[5] G.T. Kalghatgi, Fuel Anti-Knock Quality- Part II. Vehicle Studies - How Relevant is Motor Octane Number (MON) in Modern Engines?, in: SAE Technical paper 2001-01-3585, 2001.

[6] G.M. Fioroni, M.J. Rahimi, C.K. Westbrook, S.W. Wagnon, W.J. Pitz, S. Kim, R.L. McCormick, Chemical kinetic basis of synergistic blending for research octane number, Fuel. 307 (2022) 121865.

[7] W.J. Pitz, N.P. Cernansky, F.L. Dryer, F.N. Egolfopoulos, J.T. Farrell, D.G. Friend, H. Pitsch, Development of an experimental database and chemical kinetic models for surrogate gasoline fuels, Society of Automotive Engineers Paper. (2007) 0175.

[8] F. Battin-Leclerc, Detailed chemical kinetic models for the low-temperature combustion of hydrocarbons with application to gasoline and diesel fuel surrogates, Prog. Energy Combust. Sci. 34 (2008) 440–498.

[9] G. Vanhove, M. Ribaucour, R. Minetti, On the influence of the position of the double bond on the low-temperature chemistry of hexenes, Proceedings of the Combustion Institute. 30 (2005) 1065–1072.

[10] N. Lokachari, S. Panigrahy, G. Kukkadapu, G. Kim, S.S. Vasu, W.J. Pitz, H.J. Curran, The influence of iso-butene kinetics on the reactivity of di-isobutylene and iso-octane, Combustion and Flame. 222 (2020) 186–195.
[11] H.J. Curran, Gaffuri, P., Pitz, W.J., Westbrook, C.K., A comprehensive modeling study of iso-octane oxidation, Combust. Flame. 129 (2002) 253–280.
[12] N. Atef, G. Kukkadapu, S.Y. Mohamed, M.A. Rashidi, C. Banyon, M. Mehl, K.A. Heufer, E.F. Nasir, A. Alfazazi, A.K. Das, C.K. Westbrook, W.J. Pitz, T. Lu, A. Farooq, C.-J. Sung, H.J. Curran, S.M. Sarathy, A comprehensive iso-octane combustion model with improved thermochemistry and chemical kinetics, Combust. Flame. 178 (2017) 111–134.
[13] G. Kukkadapu, K. Kumar, C.-J. Sung, M. Mehl, W.J. Pitz, Autoignition of gasoline and its surrogates in a rapid compression machine, Proc. Combust. Inst. 34 (2013) 345–352.
[14] H.J. Curran, P. Gaffuri, W.J. Pitz, C.K. Westbrook, A Comprehensive Modeling Study of n-Heptane Oxidation, Combust. Flame. 114 (1998) 149–177.
[15] C.-W. Zhou, Y. Li, E. O'Connor, K.P. Somers, S. Thion, C. Keesee, O. Mathieu, E.L. Petersen, T.A. DeVerter, M.A. Oehlschlaeger, G. Kukkadapu, C.-J. Sung, M. Alrefae, F. Khaled, A. Farooq, P. Dirrenberger, P.-A. Glaude, F. Battin-Leclerc, J. Santner, Y. Ju, T. Held, F.M. Haas, F.L. Dryer, H.J. Curran, A comprehensive experimental and modeling study of isobutene oxidation, Combustion and Flame. 167 (2016) 353–379.
[16] C.K. Westbrook, W.J. Pitz, M. Mehl, P.-A. Glaude, O. Herbinet, S. Bax, F. Battin-Leclerc, O. Mathieu, E.L. Petersen, J. Bugler, H.J. Curran, Experimental and Kinetic Modeling Study of 2-Methyl-2-Butene: Allylic Hydrocarbon Kinetics, J. Phys. Chem. A. 119 (2015) 7462–7480.
[17] S.A. Alturaifi, C.R. Mulvihill, O. Mathieu, E.L. Petersen, Speciation measurements in shock tubes for validation of complex chemical kinetics mechanisms: Application to 2-Methyl-2-Butene oxidation, Combustion and Flame. 225 (2021) 196–213.
[18] C.M. Grégoire, C.K. Westbrook, S.A. Alturaifi, O. Mathieu, E.L. Petersen, Shock-tube spectroscopic water measurements and detailed kinetics modeling of 1-pentene and 3-methyl-1-butene, Int. J. Chem. Kinet. 53 (2021) 67–83.
[19] F. Arafin, A. Laich, E. Ninnemann, R. Greene, R.K. Rahman, S.S. Vasu, Influence of the double bond position in combustion chemistry of methyl butene isomers: A shock tube and laser absorption study, International Journal of Chemical Kinetics. 52 (2020) 739–751.
[20] C.M. Grégoire, C.K. Westbrook, O. Mathieu, S.P. Cooper, S.A. Alturaifi, E.L. Petersen, A Shock-Tube and Chemical Kinetics Model Investigation Encompassing all Five Pentene Isomers, Fuel. 323 (2022) 124223.
[21] S.S. Nagaraja, J. Liang, B. Liu, Q. Xu, C. Shao, G. Kukkadapu, H. Lu, Z. Wang, W.J. Pitz, S.M. Sarathy, H.J. Curran, An experimental and modeling study of tetramethyl ethylene pyrolysis with polycyclic aromatic hydrocarbon formation, Proceedings of the Combustion Institute. (2022).
[22] R. Minetti, A. Roubaud, E. Therssen, M. Ribaucour, L.R. Sochet, The chemistry of pre-ignition of n-pentane and 1-pentene, Combustion and Flame. 118 (1999) 213–220.
[23] M. Ribaucour, R. Minetti, L.R. Sochet, Autoignition of n-pentane and 1-pentene: Experimental data and kinetic modeling, Symposium (International) on Combustion. 27 (1998) 345–351.
[24] M. Mehl, W.J. Pitz, C.K. Westbrook, K. Yasunaga, C. Conroy, H.J. Curran, Autoignition behavior of unsaturated hydrocarbons in the low and high temperature regions, Proc. Combust. Inst. 33 (2011) 201–208.
[25] M. Mehl, G. Vanhove, W.J. Pitz, E. Ranzi, Oxidation and combustion of the n-hexene isomers: A wide range kinetic modeling study, Combustion and Flame. 155 (2008) 756–772.
[26] S. Touchard, R. Fournet, P.A. Glaude, V. Warth, F. Battin-Leclerc, G. Vanhove, M. Ribaucour, R. Minetti, Modeling of the oxidation of large alkenes at low temperature, Proceedings of the Combustion Institute. 30 (2005) 1073–1081.

[27] X. Meng, A. Rodriguez, O. Herbinet, T. Wang, F. Battin-Leclerc, Revisiting 1-hexene low-temperature oxidation, Combustion and Flame. 181 (2017) 283–299.
[28] Y. Wu, Y. Liu, C. Tang, Z. Huang, Ignition delay times measurement and kinetic modeling studies of 1-heptene, 2-heptene and n-heptane at low to intermediate temperatures by using a rapid compression machine, Combustion and Flame. 197 (2018) 30–40.
[29] S. Tanaka, F. Ayala, J.C. Keck, J.B. Heywood, Two-stage ignition in HCCI combustion and HCCI control by fuels and additives, Combustion and Flame. 132 (2003) 219–239.
[30] R. Bounaceur, V. Warth, B. Sirjean, P.A. Glaude, R. Fournet, F. Battin-Leclerc, Influence of the position of the double bond on the autoignition of linear alkenes at low temperature, Proceedings of the Combustion Institute. 32 (2009) 387–394.
[31] W.K. Metcalfe, W.J. Pitz, H.J. Curran, J.M. Simmie, C.K. Westbrook, The development of a detailed chemical kinetic mechanism for diisobutylene and comparison to shock tube ignition times, Proc. Combust. Inst. 31 (2007) 377–384.
[32] G. Yin, Z. Gao, E. Hu, Z. Xu, Z. Huang, Comprehensive experimental and kinetic study of 2,4,4-trimethyl-1-pentene oxidation, Combust. Flame. 208 (2019) 246–261.
[33] N. Lokachari, G. Kukkadapu, H. Song, G. Vanhove, M. Lailliau, G. Dayma, Z. Serinyel, K. Zhang, R. Dauphin, B. Etz, S. Kim, M. Steglich, A. Bodi, G. Fioroni, P. Hemberger, S.S. Matveev, A.A. Konnov, P. Dagaut, S.W. Wagnon, W.J. Pitz, H.J. Curran, A comprehensive experimental and kinetic modeling study of di-isobutylene isomers: Part 1, Combustion and Flame. (2022) 112301.
[34] H. Song, R. Dauphin, G. Vanhove, A kinetic investigation on the synergistic low-temperature reactivity, antagonistic RON blending of high-octane fuels: Diisobutylene and cyclopentane, Combustion and Flame. 220 (2020) 23–33.
[35] G. Yin, E. Hu, X. Li, J. Ku, Z. Gao, Z. Huang, Theoretical Study of Abstraction and Addition Reactions of 2,4,4-Trimethyl-1-pentene with H and O(^{3}P) Radical, Energy Fuels. 32 (2018) 11831–11842.
[36] G. Yin, E. Hu, Z. Gao, F. Yang, Z. Huang, Kinetics of H abstraction and addition reactions of 2,4,4-trimethyl-2-pentene by OH radical, Chem. Phys. Lett. 696 (2018) 125–134.
[37] J. Zádor, S.J. Klippenstein, J.A. Miller, Pressure-Dependent OH Yields in Alkene + HO_2 Reactions: A Theoretical Study, J. Phys. Chem. A. 115 (2011) 10218–10225.
[38] J. Zádor, C.A. Taatjes, R.X. Fernandes, Kinetics of elementary reactions in low-temperature autoignition chemistry, Prog. Energy Combust. Sci. 37 (2011) 371–421.
[39] G. Yin, Y. Zhao, B. Xiao, W. Jin, E. Hu, Z. Huang, Experimental and model investigation of the low temperature oxidation and pyrolysis of 2-methyl-2-butene in a jet-stirred reactor, Combustion and Flame. 242 (2022) 112174.
[40] X. You, Y. Chi, T. He, Theoretical Analysis of the Effect of C═C Double Bonds on the Low-Temperature Reactivity of Alkenylperoxy Radicals, J. Phys. Chem. A. 120 (2016) 5969–5978.
[41] D.J.M. Ray, D.J. Waddington, Gas phase oxidation of alkenes—Part II. The oxidation of 2-methylbutene-2 and 2,3-dimethylbutene-2, Combust. Flame. 20 (1973) 327–334.
[42] C.M. Grégoire, C.K. Westbrook, S.P. Cooper, M.A. Turner, S.A. Alturaifi, O. Mathieu, E.L. Petersen, Laminar Flame Speed, Ignition Delay Time, and CO Laser Absorption Measurements of a Gasoline-like Blend of Pentene Isomers, J. Phys. Chem. A. (2023).
[43] N. Lokachari, G. Kukkadapu, B. Etz, G. Fioroni, S. Kim, M. Steglich, A. Bodi, P. Hemberger, S.S. Matveev, A. Thomas, H. Song, G. Vanhove, K. Zhang, G. Dayma, M. Lailliau, Z. Serinyel, A.A. Konnov, P. Dagaut, W.J. Pitz, H.J. Curran, A comprehensive experimental and kinetic modeling study of di-isobutylene isomers: Part 2, Combustion and Flame. (n.d.) in press.
[44] J.T. Scanlon, D.E. Willis, Calculation of Flame Ionization Detector Relative Response Factors Using the Effective Carbon Number Concept, J. Chromatogr. Sci. 23 (1985) 333–340.

[45] Goldsborough, S. Scott., Hochgreb, Simone., Vanhove, Guillaume., Wooldridge, Margaret S., Curran, Henry J., Sung, Chih-Jen, Advances in rapid compression machine studies of low- and intermediate-temperature autoignition phenomena, Prog. Energy Combust. Sci. 63 (2017) 1–78.
[46] D. Lee, S. Hochgreb, Rapid Compression Machines: Heat Transfer and Suppression of Corner Vortex, Combustion and Flame. 114 (1998) 531–545.
[47] N. Bourgeois, S.S. Goldsborough, H. Jeanmart, F. Contino, CFD simulations of Rapid Compression Machines using detailed chemistry: Evaluation of the 'crevice containment' concept, Combust. Flame. 189 (2018) 225–239.
[48] G. Mittal, C.-J. Sung, Homogeneous charge compression ignition of binary fuel blends, Combust. Flame. 155 (2008) 431–439.
[49] C.-J. Sung, H.J. Curran, Using rapid compression machines for chemical kinetics studies, Prog. Energy Combust. Sci. 44 (2014) 1–18.
[50] C.S. Mergulhão, H.-H. Carstensen, H. Song, S.W. Wagnon, W.J. Pitz, G. Vanhove, Probing the antiknock effect of anisole through an ignition, speciation and modeling study of its blends with isooctane, Proceedings of the Combustion Institute. 38 (n.d.) in press.
[51] A. Fridlyand, S.S. Goldsborough, M. Al Rashidi, S.M. Sarathy, M. Mehl, W.J. Pitz, Low temperature autoignition of 5-membered ring naphthenes: Effects of substitution, Combust. Flame. 200 (2019) 387–404.
[52] N. Bourgeois, H. Jeanmart, G. Winckelmans, O. Lamberts, F. Contino, How to ensure the interpretability of experimental data in Rapid Compression Machines? A method to validate piston crevice designs, Combustion and Flame. 198 (2018) 393–411.
[53] C.M. Grégoire, C.K. Westbrook, G. Kukkadapu, S.P. Cooper, S.A. Alturaifi, O. Mathieu, E.L. Petersen, Shock-tube spectroscopic CO and H2O measurements during 2-methyl-1-butene combustion and chemical kinetics modeling, Combustion and Flame. 238 (2022) 111919.
[54] J. Zádor, A.W. Jasper, J.A. Miller, The reaction between propene and hydroxyl, Phys. Chem. Chem. Phys. 11 (2009) 11040–11053.
[55] J.C. Lizardo-Huerta, B. Sirjean, R. Bounaceur, R. Fournet, Intramolecular effects on the kinetics of unimolecular reactions of β-HOROO˙ and HOQ˙OOH radicals, Phys. Chem. Chem. Phys. 18 (2016) 12231–12251.
[56] S. Dong, K. Zhang, E.M. Ninnemann, A. Najjar, G. Kukkadapu, J. Baker, F. Arafin, Z. Wang, W.J. Pitz, S.S. Vasu, S.M. Sarathy, P.K. Senecal, H.J. Curran, A comprehensive experimental and kinetic modeling study of 1- and 2-pentene, Combustion and Flame. 223 (2021) 166–180.
[57] J. Bugler, K.P. Somers, E.J. Silke, H.J. Curran, Revisiting the Kinetics and Thermodynamics of the Low-Temperature Oxidation Pathways of Alkanes: A Case Study of the Three Pentane Isomers, The Journal of Physical Chemistry A. 119 (2015) 7510–7527.
[58] C. Cavallotti, F. Leonori, N. Balucani, V. Nevrly, A. Bergeat, S. Falcinelli, G. Vanuzzo, P. Casavecchia, Relevance of the Channel Leading to Formaldehyde + Triplet Ethylidene in the O(3P) + Propene Reaction under Combustion Conditions, J. Phys. Chem. Lett. 5 (2014) 4213–4218.
[59] J. Power, K.P. Somers, S.S. Nagaraja, W. Wyrebak, H.J. Curran, Theoretical Study of the Reaction of Hydrogen Atoms with Three Pentene Isomers: 2-Methyl-1-butene, 2-Methyl-2-butene, and 3-Methyl-1-butene, J Phys Chem A. 124 (2020) 10649–10666.
[60] R. Fang, G. Kukkadapu, M. Wang, S.W. Wagnon, K. Zhang, M. Mehl, C.K. Westbrook, W.J. Pitz, C.-J. Sung, Fuel molecular structure effect on autoignition of highly branched iso-alkanes at low-to-intermediate temperatures: Iso-octane versus iso-dodecane, Combustion and Flame. 214 (2020) 152–166.
[61] C.-W. Zhou, J.M. Simmie, K.P. Somers, C.F. Goldsmith, H.J. Curran, Chemical Kinetics of Hydrogen Atom Abstraction from Allylic Sites by 3O2; Implications for Combustion Modeling and Simulation, J. Phys. Chem. A. 121 (2017) 1890–1899.

[62] S.S. Vasu, L.K. Huynh, D.F. Davidson, R.K. Hanson, D.M. Golden, Reactions of OH with Butene Isomers: Measurements of the Overall Rates and a Theoretical Study, J. Phys. Chem. A. 115 (2011) 2549–2556.
[63] S.M. Burke, U. Burke, R. Mc Donagh, O. Mathieu, I. Osorio, C. Keesee, A. Morones, E.L. Petersen, W. Wang, T.A. DeVerter, M.A. Oehlschlaeger, B. Rhodes, R.K. Hanson, D.F. Davidson, B.W. Weber, C.-J. Sung, J. Santner, Y. Ju, F.M. Haas, F.L. Dryer, E.N. Volkov, E.J.K. Nilsson, A.A. Konnov, M. Alrefae, F. Khaled, A. Farooq, P. Dirrenberger, P.-A. Glaude, F. Battin-Leclerc, H.J. Curran, An experimental and modeling study of propene oxidation. Part 2: Ignition delay time and flame speed measurements, Combustion and Flame. 162 (2015) 296–314.
[64] C.-J. Chen, J.W. Bozzelli, Thermochemical Property, Pathway and Kinetic Analysis on the Reactions of Allylic Isobutenyl Radical with O_2 : an Elementary Reaction Mechanism for Isobutene Oxidation, The Journal of Physical Chemistry A. 104 (2000) 9715–9732.
[65] E. Grajales-González, G. Kukkadapu, S.S. Nagaraja, C. Shao, M. Monge-Palacios, J.E. Chavarrio, S.W. Wagnon, H.J. Curran, W.J. Pitz, S. Mani Sarathy, An experimental and kinetic modeling study of the pyrolysis of isoprene, a significant biogenic hydrocarbon in naturally occurring vegetation fires, Combustion and Flame. 242 (2022) 112206.
[66] C.F. Goldsmith, S.J. Klippenstein, W.H. Green, Theoretical rate coefficients for allyl+HO2 and allyloxy decomposition, Proceedings of the Combustion Institute. 33 (2011) 273–282.
[67] C.F. Goldsmith, W.H. Green, S.J. Klippenstein, Role of O2 + QOOH in Low-Temperature Ignition of Propane. 1. Temperature and Pressure Dependent Rate Coefficients, J. Phys. Chem. A. 116 (2012) 3325–3346.
[68] G. da Silva, J.W. Bozzelli, Kinetics of the benzyl + O(3P) reaction: a quantum chemical/statistical reaction rate theory study, Phys. Chem. Chem. Phys. 14 (2012) 16143–16154.
[69] K. Wang, S.M. Villano, A.M. Dean, Reactivity–Structure-Based Rate Estimation Rules for Alkyl Radical H Atom Shift and Alkenyl Radical Cycloaddition Reactions, J. Phys. Chem. A. 119 (2015) 7205–7221.
[70] A. Fridlyand, P.T. Lynch, R.S. Tranter, K. Brezinsky, Single pulse shock tube study of allyl radical recombination, J Phys Chem A. 117 (2013) 4762–4776.
[71] X. Chen, C.F. Goldsmith, A Theoretical and Computational Analysis of the Methyl-Vinyl + O2 Reaction and Its Effects on Propene Combustion, J. Phys. Chem. A. 121 (2017) 9173–9184.
[72] K. Wang, S.M. Villano, A.M. Dean, Fundamentally-based kinetic model for propene pyrolysis, Combustion and Flame. 162 (2015) 4456–4470.
[73] D.G. Goodwin, H.K. Moffat, R.L. Speth, Cantera: An object-oriented software toolkit for chemical kinetics, thermodynamics, and transport processes., (2018).
[74] S. Cheng, D. Kang, A. Fridlyand, S.S. Goldsborough, C. Saggese, S. Wagnon, M.J. McNenly, M. Mehl, W.J. Pitz, D. Vuilleumier, Autoignition behavior of gasoline/ethanol blends at engine-relevant conditions, Combustion and Flame. 216 (2020) 369–384.
[75] Y. Fenard, M.A. Boumehdi, G. Vanhove, Experimental and kinetic modeling study of 2-methyltetrahydrofuran oxidation under engine-relevant conditions, Combustion and Flame. 178 (2017) 168–181.
[76] B.-J. Zhong, Z.-M. Zeng, H.-S. Peng, The pressure dependence of laminar flame speed of 2-methyl-2-butene/air flames in the 0.1–1.0 MPa range, Combustion Science and Technology. 190 (2018) 1886–1899.